Journal of Nuclear Materials 379 (2008) 154–161

Contents lists available at ScienceDirect

Journal of Nuclear Materials

journal homepage: www.elsevier.com/locate/jnucmat

Influence of sulfide concentration on the corrosion behavior of pure copper in synthetic seawater

Naoki Taniguchi [a,*], Manabu Kawasaki[b]

[a] Japan Atomic Energy Agency (JAEA), Tokai-mura, Ibaraki 319-1194, Japan
[b] Inspection Development Corporation, Japan

A B S T R A C T

Corrosion rate and stress corrosion cracking (SCC) behavior of pure copper under anaerobic conditions were studied by immersion tests and slow strain rate tests (SSRT) in synthetic seawater containing Na_2S. The corrosion rate was increased with sulfide concentration both in simple saline solution and in bentnite–sand mixture. The results of SSRT showed that copper was susceptible to intergranular attack; selective dissolution at lower sulfide concentration (less than 0.005 M) and SCC at higher sulfide concentration (0.01 M). It was expected that if the sulfide concentration in groundwater is less than 0.001 M, pure copper is possible to exhibit superior corrosion resistance under anaerobic condition evident by very low corrosion rates and immunity to SCC. In such a low sulfide environment, copper overpack has the potential to achieve super-long lifetimes exceeding several tens of thousands years according to long-term simulations of corrosion based on diffusion of sulfide in buffer material.

1. Introduction

Overpack is one component of the engineered barrier system for high-level radioactive waste disposal, and is required to prevent the contact of groundwater with vitrified waste for at least 1000 years [1]. In Japan, carbon steel, titanium and copper have been selected as candidate overpack materials [1]. Among these metals, copper is the only one that has thermodynamic stability under anaerobic conditions [2]. This property is a convincing indication of long-term integrity of overpack against groundwater in deep, essentially anaerobic underground environments. Sulfide, however, is known to corrode copper to Cu_2S due to the reduction of H_2O in an anaerobic environment [3].

Fig. 1 shows the corrosion scenario for copper overpack from burial to initial failure. The conditions in the initial post-closure phase will be relatively aerobic due to introduction of oxygen during excavation and construction of the repository. Under such conditions, the reduction of oxygen will dominate the cathodic reaction and corrosion will be either general or localized, depending on the environmental conditions. The oxygen will be consumed by corrosion or reaction with minerals such as pyrite in bentonite buffer material emplaced around the overpack. After the consumption of oxygen, anaerobic conditions will exist around the overpack. If sulfide is not present in water in contact with the overpack, design corrosion limits will not be exceeded and copper overpacks could possibly achieve a very long lifetime due to thermodynamic stability.

On the other hand, if sulfide such as H_2S, HS^- and S^{2-} present in water comes into contact with the overpack, copper will corrode and water will eventually penetrate the overpack sooner or later, depending on the corrosion rate. Various studies using electrochemical techniques or immersion tests up to several days duration [4–7] have been conducted on corrosion of copper due to sulfide, but previous experimental studies have focused only on the early stages of corrosion. In this study, we studied the corrosion behavior in sulfide environments using long-term immersion tests of up to 730 days duration, and determined corrosion rates and their dependency on sulfide concentration. In addition to these experimental studies, long-term prediction of corrosion depth due to sulfide was also done and the possibility of achieving super-long lifetimes far exceeding 1000 years is discussed.

Another concern related to corrosion due to sulfide is the initiation of stress corrosion cracking (SCC). Selection of copper as overpack material should be done after clarification of the susceptibility to SCC, because SCC propagation rate is generally very high. In spite of the large impact of SCC on the long term integrity of copper overpack, there are few studies on the behavior of SCC due to sulfide. In this study, the SCC susceptibility in a sulfide rich environment was investigated by slow strain rate tests (SSRT) as a preliminary study to estimate approximately the lower limit of sulfide concentration for initiation of SCC.

* Corresponding author. Tel.: +81 29 282 1111; fax: +81 29 282 9328.
E-mail address: taniguchi.naoki@jaea.go.jp (N. Taniguchi).

0022-3115/$ - see front matter © 2008 Elsevier B.V. All rights reserved.
doi:10.1016/j.jnucmat.2008.06.010

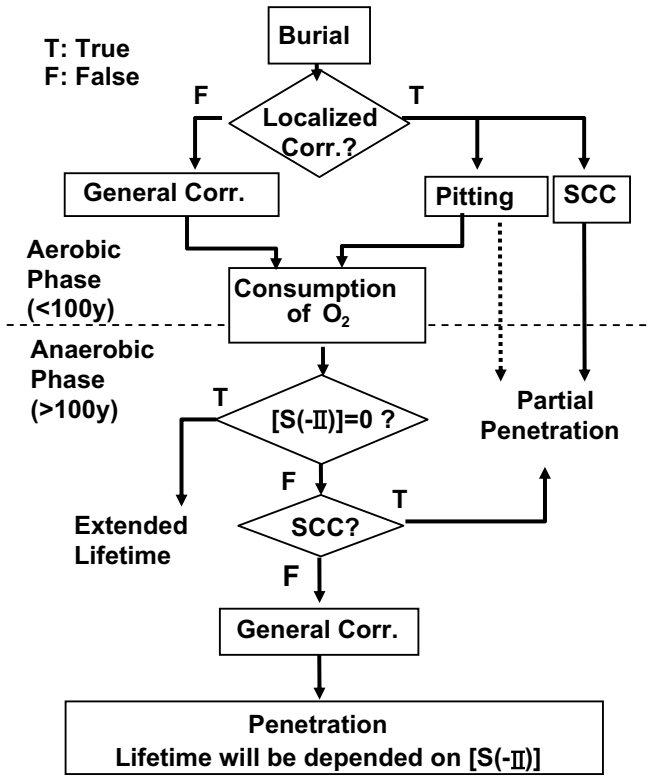

Fig. 1. Corrosion scenario of copper overpack from burial to failure.

2. Experimental

2.1. Immersion tests

Oxygen free copper of >99.99% purity, in conformity with Japanese industrial standards JIS C1020P, was used in the immersion tests. The copper was cut into 30 mm square, 2 mm thick coupons and surfaces were polished with 3 μm, micro grit diamond paste and rinsed with acetone.

Since relatively high sulfide concentrations are expected in saline groundwater [8], synthetic seawater (SSW) was selected as the test solution and Na_2S was added. The chemical composition of the test solutions and pH are shown in Table 1. The immersion tests were conducted in simple saline solutions and using bentonite-sand mixtures in saline solutions to simulate buffer material. The bentonite was sodium type (Kunigel-V1) and the mixing ratio of the bentonite to sand was 7 to 3, the reference design ratio for the engineered barrier system [1]. The bentonite–sand mixture was compacted in a titanium column with the copper coupons to a dry density of 1.6 Mg/m^3 following the reference design of buffer material in Japanese program [1]. The details of the test method using the column for immersion tests in bentonite-sand mixtures were described in a previous study [9].

Table 1
Chemical composition and pH of synthetic seawater

Component	Concentration (M)	Component	Concentration (M)
Cl^-	5.6×10^{-1}	Na^+	4.8×10^{-1}
SO_4^{2-}	2.9×10^{-2}	K^+	1.0×10^{-2}
HCO_3^-	2.4×10^{-3}	Ca^+	1.0×10^{-2}
F^-	7.4×10^{-5}	Mg^{2+}	5.5×10^{-2}
Br^-	8.6×10^{-4}	Sr^{2+}	7.0×10^{-4}
BO_3^-	4.4×10^{-4}	pH	7.9–8.4

The coupons, titanium columns and test solutions were placed in an N_2 atmosphere glove box in which oxygen gas concentration was controlled to less than 1 ppm. The test solution was deaerated by purging N_2 gas in the glove box for over 24 h. The Na_2S was added to the test solution after the deaeration of the test solution in order to prevent the release of sulfide from the solution during the N_2 gas purging. The trapped air in bentonite-sand mixture was removed by evacuation for over 24 h in the glove box, and then replaced by N_2 gas. By removing the trapped air, it can be assumed that the pore of bentonite-sand mixture was anaerobic condition and that the change of sulfide concentration due to the oxidation of S(-II) to S(VI) by trapped oxygen was quite small. The coupons and test columns were placed in PTFE containers and the test solutions were poured in. The screw top of the container was tightly occluded with PTFE sealing tape, and then the container was placed in a constant temperature oven attached to the glove box.

The temperature was kept at 353 K simulating the relatively high temperature condition at the overpack surface. The immersion test durations were 30, 90 and 365 days for the tests in simple solution, and 30, 90, 180, 365 and 730 days for the tests with the bentonite-sand mixtures. After the immersion periods, the copper coupons were extracted from the simple solution and the bentonite–sand mixture. The coupons were chemically cleaned in KCl–HCl solution and mass losses of the coupons were determined to estimate the amount of corrosion. The surface of one of the coupons was analyzed by X-ray diffraction (XRD) to identify the corrosion products and then examined using a scanning electron microscope (SEM).

2.2. Slow strain rate tests (SSRT)

Phosphorous–deoxidized copper used in trial manufacture of copper overpack [10] was selected as the coupon material. The chemical impurities in the copper are shown in Table 2, and the geometry of the coupon is shown in Fig. 2. The coupon surfaces were polished with 3 μm, micro grit diamond paste prior to the SSRT.

Table 2
Chemical composition of copper coupons used for slow strain rate tests

Element	Content (ppm)
Pb	1.9
Zn	<1
Bi	<1
Cd	<1
Hg	<1
O	3.0
P	45
S	<1
Se	<1
Te	<1
H	0.4
Cu	Balance

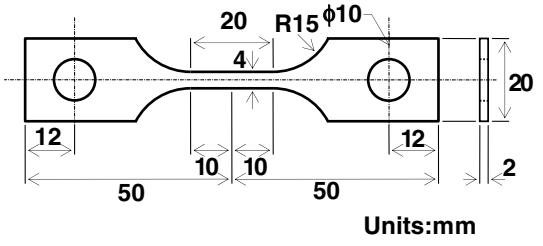

Fig. 2. Geometry of coupons for the slow strain rate tests.

The SSRT were conducted in synthetic seawater (Table 1) containing Na_2S at 353 K as was used for the immersion tests. The sulfide concentrations were 0.0 M, 0.001 M, 0.005 M and 0.01 M, respectively. In addition, tests in silicone oil were also carried out at the same temperature and strain rate to compare the behavior in an inert environment. A uniaxial tensile test machine equipped with an electrochemical cell consisting of glass was used for the SSRT, and saturated calomel electrodes (SCE) and platinum counter-electrodes were attached to the cell to control electrochemical potential of coupons. The electrode potential was fixed at the rest potential value in an N_2 atmosphere measured under the same conditions in advance of the SSRT. The rest potentials in synthetic seawater containing Na_2S were: –450 mV vs. SCE for 0 M; −880 mV vs. SCE for 0.001 M; −920 mV vs. SCE for 0.005 M; and −950 mV vs. SCE for 0.01 M.

Coupons were strained to fracture at a constant extension rate of 8.3×10^{-7}/s, which is an ordinary extension rate in the SSRT [11,12]. The test solutions in the cell were renewed every few days, 3 days maximum, during the SSRTs in order to avoid decreased sulfide concentration, since the test cells were not designed to be completely airtight and could allow the partial leakage of sulfide as H_2S gas. After failure, the coupons were chemically cleaned in KCl–HCl solution and the coupon surfaces were examined using a scanning electron microscope (SEM). In order to observe crack growth and determine the fracture type, cross-sectional observations were also performed.

3. Results and discussion

3.1. Corrosion product and corrosion rate

Optical photographs of the coupons after the 365 day immersion tests in 0.1 M-Na_2S shown in Fig. 3 are representative of surface appearance. The surface was uniformly covered with black corrosion products and no indication of localized corrosion was found on the surface in both simple solution and for the bentonite–sand mixture. While there is no remarkable deference between simple solution and bentonite–sand mixture in the color of the corrosion products and in the corrosion form, the degree of the adhesion of corrosion products to the coupon surface was very different between them. The corrosion products formed in simple solution adhered strongly to the coupon surfaces, whereas those in the bentonite–sand mixture were easily separated from the surface and bare metal was partially exposed during removal of the coupon from the test column. The SEM photomicrographs of coupon surfaces after the immersion tests are shown in Fig. 4. In tests with 0.0 M Na_2S, only polishing patterns were observed and no perceptible corrosion products were found on the surfaces in either the simple solutions or in the bentonite–sand mixture. As for the tests with Na_2S, corrosion products formed on the surface, and they were thicker with increasing Na_2S concentration. The corrosion products formed in simple solution crystallized with particle sizes of ten or less microns. Crystalline corrosion products were also observed in the bentonite–sand mixtures saturated in 0.1 M-Na_2S solution. The particle sizes were larger than corrosion products in simple solution. As a typical example of the XRD analysis, the XRD pattern for the coupon immersed for 365 days is shown in Fig. 5. The crystalline corrosion product in almost all test cases containing Na_2S was identified as chalcocite, Cu_2S. The results of XRD analysis for every test case are summarized in Table 3.

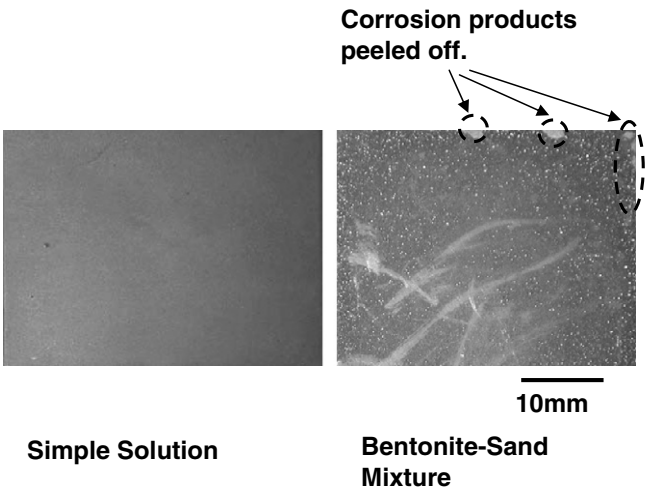

Fig. 3. Examples of optical photographs of coupon surfaces after 365 day immersion tests in 0.1 M-Na_2S.

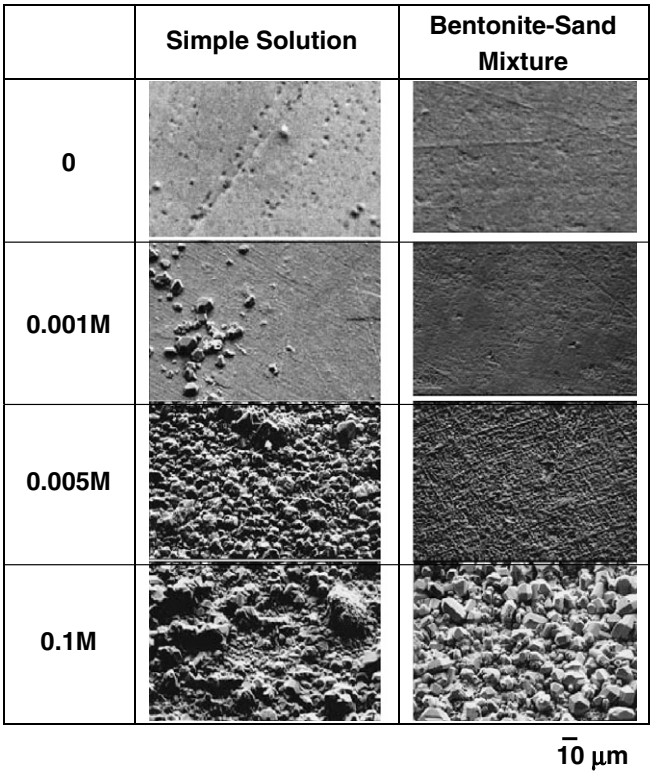

Fig. 4. SEM photomicrographs of coupon surfaces after 365 day immersion tests.

The average corrosion depth calculated from the mass losses of the coupons are shown in Fig. 6 as a function of time, and were approximated with a linear equation using the least squares method. The corrosion rates were calculated from the gradient of the line of best fit and are shown in this figure. In the 0.0 M-Na_2S and 0.001 M-Na_2S simple solutions, no significant corrosion propagation was observed; consequently the corrosion rates are estimated to be nearly zero. As the sulfide concentration increased, corrosion rates increased to 3.8 μm/y for the 0.005 M and 9.7 μm/y for the 0.1 M solutions. Similarly, the corrosion rates in bentonite–sand mixtures tended to increase with sulfide concentration. The corrosion rates in bentonite–sand mixtures seemed to be slightly larger than those in simple solution, even though the magnitude and dependence on sulfide concentration were similar to those in simple solution. From the propagation behavior of average corrosion depth, it can be summarized that the corrosion rate of pure copper is likely to be extremely small (nearly zero or less than 1 μm/y) if the sulfide concentration is less than 0.001 M.

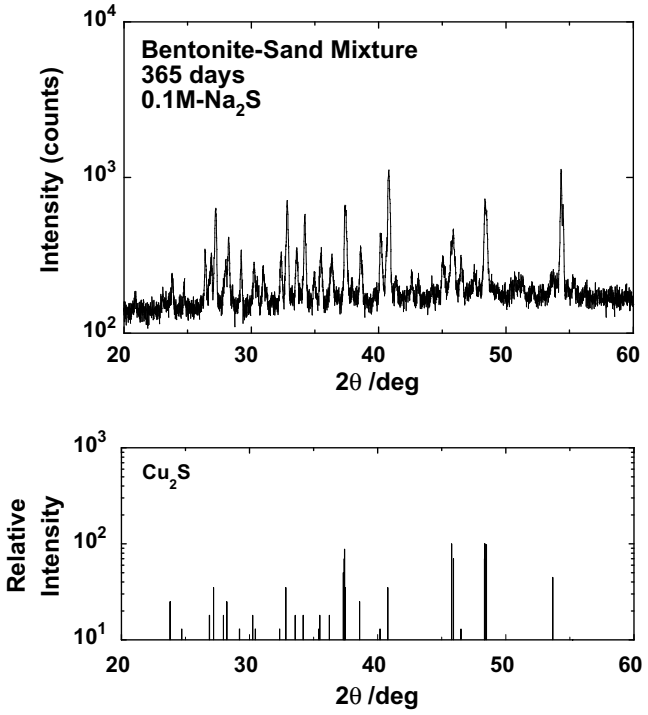

Fig. 5. XRD patterns of surface corrosion products formed in 0.1 M-Na_2S after 365 days and standard peak of chalcocite, Cu_2S.

Table 3
Corrosion products of copper identified by XRD

	Na_2S (M)	Corrosion products
Simple solution	0	Cu_2O(Cuprite)
	0.001	Cu_2S(Chalcocite)
	0.005	Cu_2S(Chalcocite), Cu_2O(Cuprite)
	0.1	Cu_2S(Chalcocite)
Bentonite–sand mixture	0	Cu_2O(Cuprite)
	0.001	Cu_2S(Chalcocite), Cu_2O(Cuprite)
	0.005	Cu_2S(Chalcocite)
	0.1	Cu_2S(Chalcocite)

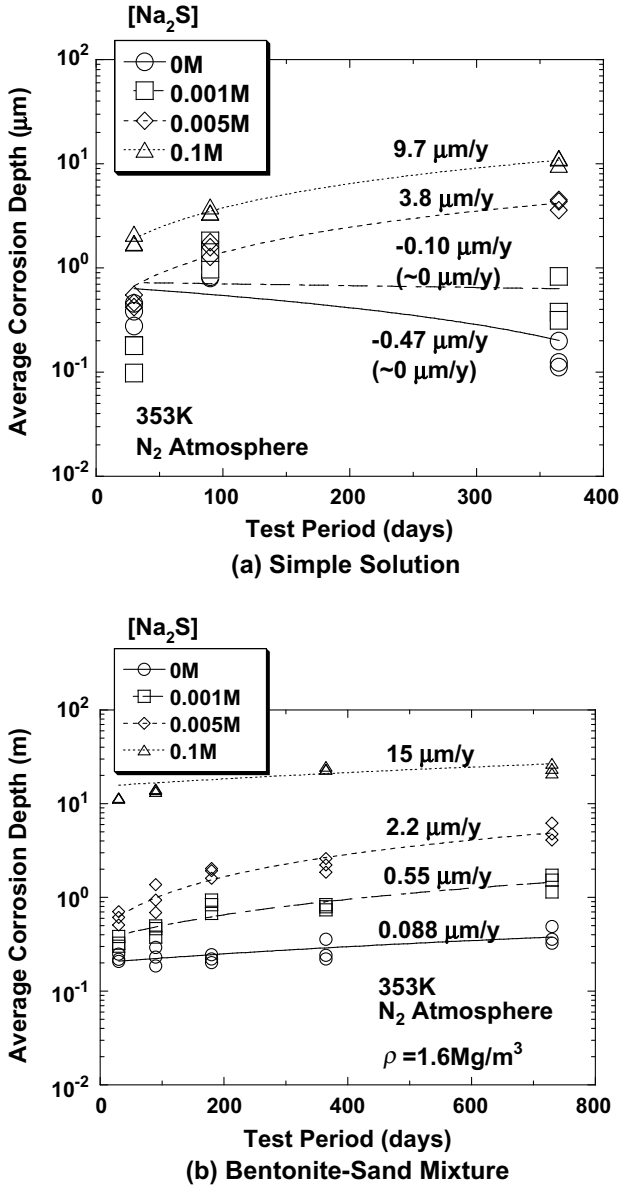

Fig. 6. Corrosion propagation in pure copper and estimated corrosion rates in synthetic sea water containing sulfide.

The corrosion rates shown in Fig. 6 were much smaller than the values estimated by an electrochemical approach or from short-term immersion tests in previous studies [4–7]. For example, Escobar et al. estimated the corrosion rates to be 27 μm/y for 0.001 M-Na_2S and 87 μm/y for 0.1 M-Na_2S based on anodic and cathodic polarization curves of pure copper in synthetic groundwater containing various Na_2S concentrations [6]. These values can be regarded as initial corrosion rates for bare metal. It can be presumed that the corrosion rate of pure copper is self-limiting as corrosion propagates. One of the important factors controlling corrosion rate is assumed to be the formation of corrosion product film. As mentioned above, very tight corrosion product film formed on the coupons immersed in simple solution and seemed to protect the surface from continued corrosion. Lower corrosion rates than those observed in previous studies are assumed to be due to the occurrence of protective corrosion product film in the simple solution cases. On the other hand, the state of surface corrosion products in bentonite–sand mixtures were obviously different from those in simple solution and seemed to be less protective. In spite of this situation, the corrosion rates were similar to those in simple solution. This indicates that the mechanism controlling the corrosion rate in bentonite-sand mixture is probably different from that in simple solution. Except for the effect of the corrosion products, some other factor is assumed to control the corrosion rate. One possible factor could be the limitation of sulfide supply to the coupon surface through the bentonite–sand mixture. Because of the low permeability of water in saturated, compacted bentonite [1], mass transport is controlled by diffusion. Therefore, it is possible that the corrosion was limited by the diffusion rate of sulfide in the bentonite-sand mixtures. King et al. also pointed out that the corrosion rate of copper in compacted bentonite is controlled by the rate of sulfide supply based on experimental results; the response of rest potential, E_{corr}, to the addition of sulfide in bentonite was far slower than that in simple solution due to restricted mass-transport in compacted bentonite [13]. In this study, we modeled the corrosion propagation based on the diffusion of sulfide in bentonite–sand mixture and compared with experimental results. The schematic of the model is illustrated in Fig. 7. One dimensional Cartesian coordinates were applied to describe the corrosion system in the bentonite-sand mixture with a thickness l (=6 mm). The boundary condition of sulfide concentration, C_1, at the interface of bulk solution and bentonite-sand mixture, $x = 0$, was fixed at 0.001 M,

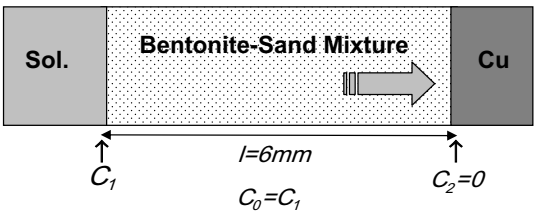

Fig. 7. Schematic of model for prediction of corrosion depth of copper based on the diffusion of HS^- in bentonite–sand mixture layer.

0.005 M and 0.1 M simulating the experimental conditions. It was assumed that the sulfide concentration, C_2, at the surface of copper, $x = l$, could be approximated as zero. The initial condition, C_0, was assumed equal to C_1. The total flux, Q, of sulfide at time, t, can be expressed by the following equation [14]:

$$Q = D\frac{(C_1 - C_2)t}{l} + \frac{2l}{\pi^2} \times \sum_{n=1}^{\infty}\left\{\frac{C_1\cos n\pi - C_2}{n^2}\left(1 - \exp\frac{-Dn^2\pi^2 t}{l^2}\right)\right\} + \frac{4C_0 l}{\pi^2} \times \sum_{m=0}^{\infty}\left[1 - \exp\left\{\frac{-D(2m+1)^2\pi^2 t}{l^2}\right\}\right]\frac{1}{(2m+1)^2}, \quad (1)$$

where D is the diffusion coefficient of sulfide in the bentonite–sand mixture. Since there is no available D value for sulfide, HS^- in bentonite–sand mixture of dry density 1.6 Mg/m^3 with 30% sand, the value of 4×10^{-11} m^2/s for Cl^- and I^- [15] was used as the value for mono-valent anions. These diffusion coefficients were corrected to the values at 353 K to be 1.0×10^{-10} m^2/s using an Arrhenius type equation and corresponding activation energy of 15.05 kJ/mol [16]. The total sulfide flux was converted into average corrosion depth assuming the corrosion reaction; $2Cu + HS^- + H^+ = Cu_2S + H_2$. The predicted average corrosion depth and comparison with experimental results are shown in Fig. 8. The predicted corrosion depths were larger than experimental results in every case. Although the

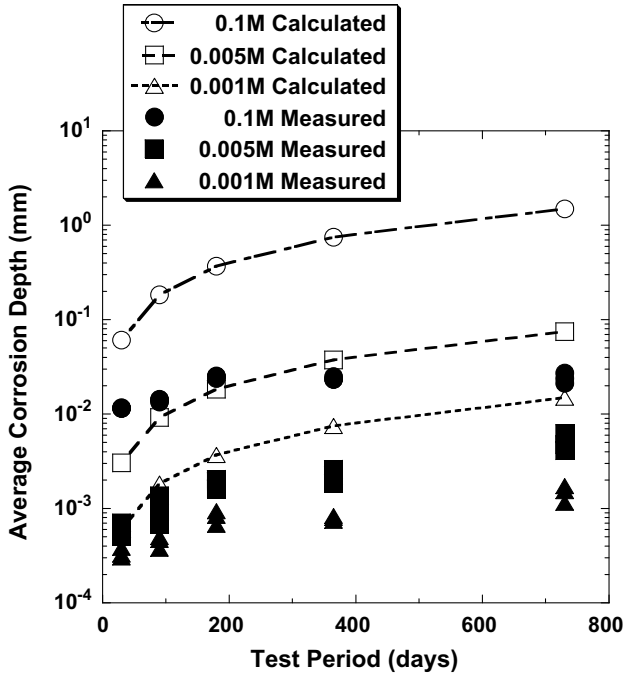

Fig. 8. Comparison of the calculated average corrosion depths in bentonite–sand mixtures with experimental results.

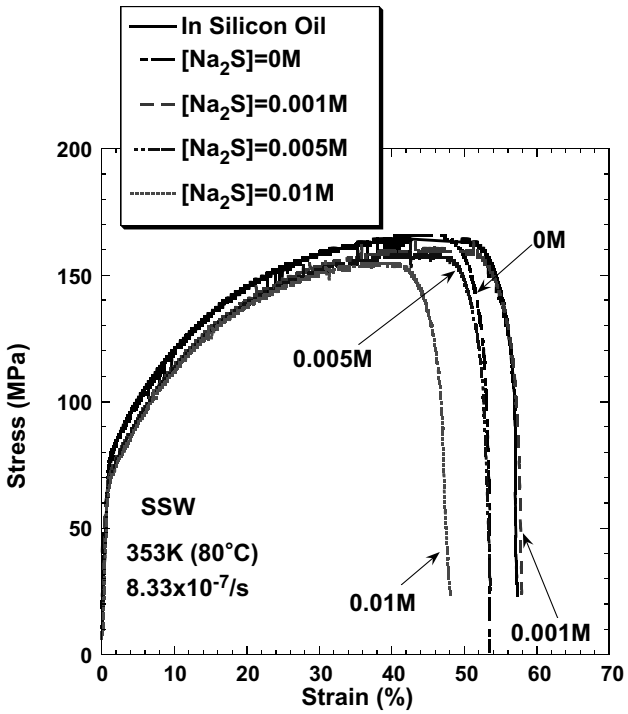

Fig. 9. Influence of sulfide concentration on the stress–strain curve of pure copper.

reason for such differences have not been clarified yet, it is possible that the corrosion products, which seem to be less protective, controlled the progress of corrosion to some degree. Although more detailed mechanisms should be considered in addition to the diffusion coefficient of sulfide in bentonite, the simulation based on the diffusion of sulfide is likely to generate a conservative assessment. The long-term prediction of corrosion of copper overpack due to sulfide is described later.

3.2. Stress corrosion cracking behavior

The stress-strain curves obtained by SSRT are shown in Fig. 9. The influence of sulfide on the curve was not definitive up to 0.005 M, whereas distinct decrease of maximum stress and strain to failure was observed at the higher sulfide concentration of 0.01 M. Fig. 10 shows the SEM photomicrographs of coupon surfaces near the fractured location after the SSRT. No cracks or selective metal dissolution were found on the coupon surfaces in the tests in silicone oil and in 0.0 M-Na_2S solution. This result shows that crack or local attack is not likely to be initiated on the coupon surface in inert environment and in sulfide free environment during SSRT. In sulfide environment, copper coupons were attacked by selective dissolution or SCC. For 0.001 M-Na_2S, a few narrow slits were observed near the fractured location and seemed to be along slip lines or grain boundaries, but were not able to be classified into neither SCC nor selective dissolution. At the higher Na_2S concentration of 0.005 M, some crevasses suspected to be SCC were observed near the fractured location. In the case of the much higher Na_2S concentration of 0.01 M, numerous, obvious cracks were observed over the coupon surface. Fig. 11 shows the results of cross sectional observations near the fractured location where indications of cracking or selective dissolution were observed. In the case of 0.001 M solutions, although the initiations of micro cracks were indicated on the surface, it seems to have propagated as intergranular corrosion rather than SCC. As for 0.005 M, concave pitting was observed and it was not likely SCC but a kind of selective dissolution. Typical SCC was observed in the tests in 0.01 M solutions and

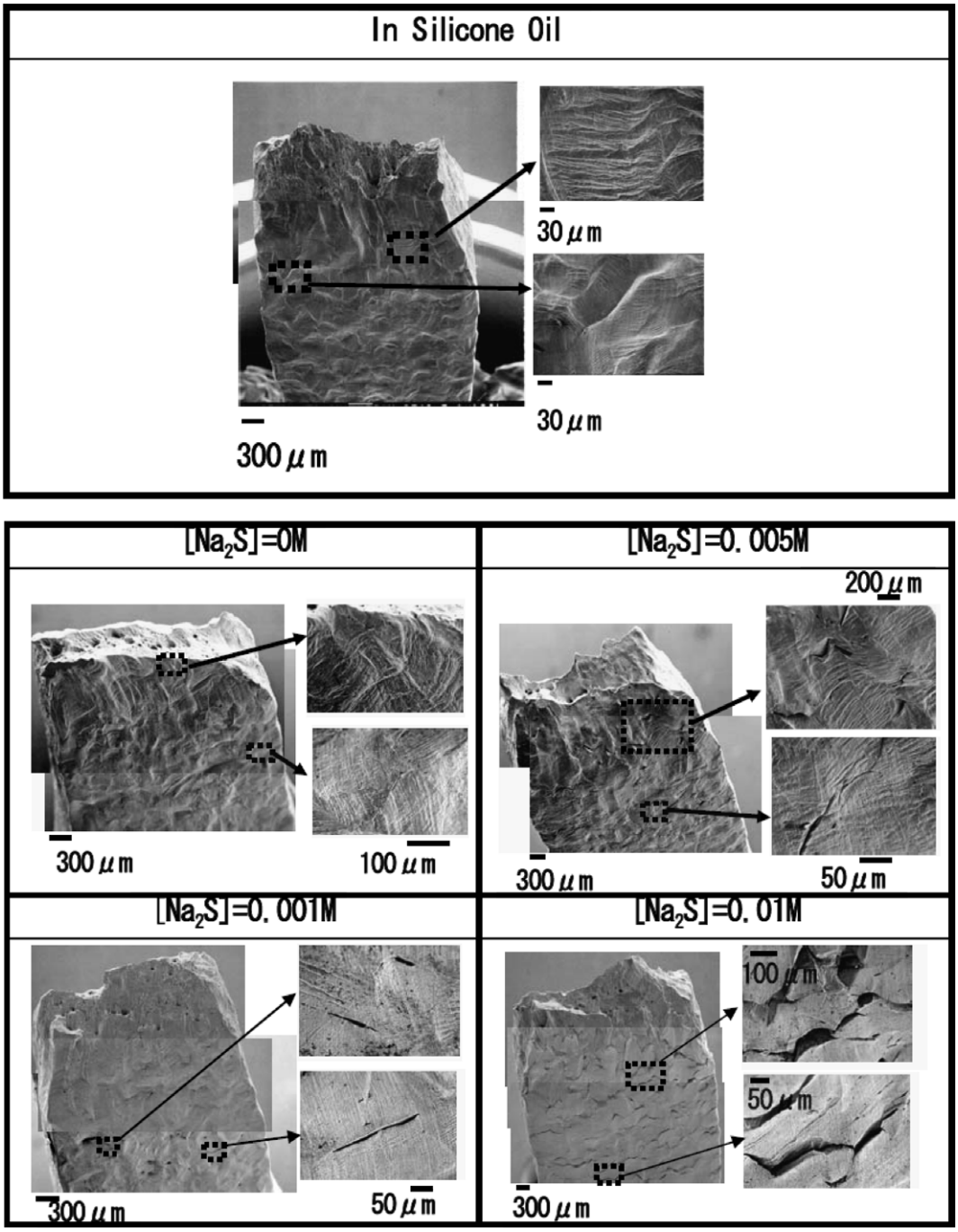

Fig. 10. SEM microphotographs of coupon surfaces after SSRT tests.

seems to have propagated along grain boundaries, therefore, the SCC mode for phosphorous–deoxidized copper in a sulfide environment is assumed to be an intergranular type. From the cross sectional observations, the slits or crevasses observed by SEM for 0.001 M and 0.005 M solutions were not attributable to SCC. Such an interpretation agreed with the stress-strain curve behavior such that obvious reduction in ductility did not appear up to 0.005 M.

It can be summarized that copper is susceptible to intergranular attack by sulfide such as selective dissolution at lower sulfide concentration and SCC at higher sulfide concentration. The threshold of sulfide concentration for SCC initiation is likely to be in the range of 0.005–0.01 M under our experimental condition. The critical sulfide concentration is possibly depends on environmental conditions (coexisting anions, electrode potential, temperature and so on) and material conditions (impurities, thermal effects, microstructures and so on). Further study is required to clear the effect of these factors, as well as the mechanism of intergranular attack.

3.3. Long-term prediction of the corrosion depth due to sulfide

As discussed above, copper is assumed to exhibit superior corrosion resistance under anaerobic conditions if the sulfide concentration is less than 0.001 M indicated by the very low corrosion rate and absence of SCC. In order to estimate the lifetime of copper overpack as a function of sulfide concentration, the long-term corrosion depth was predicted based on the model discussed in

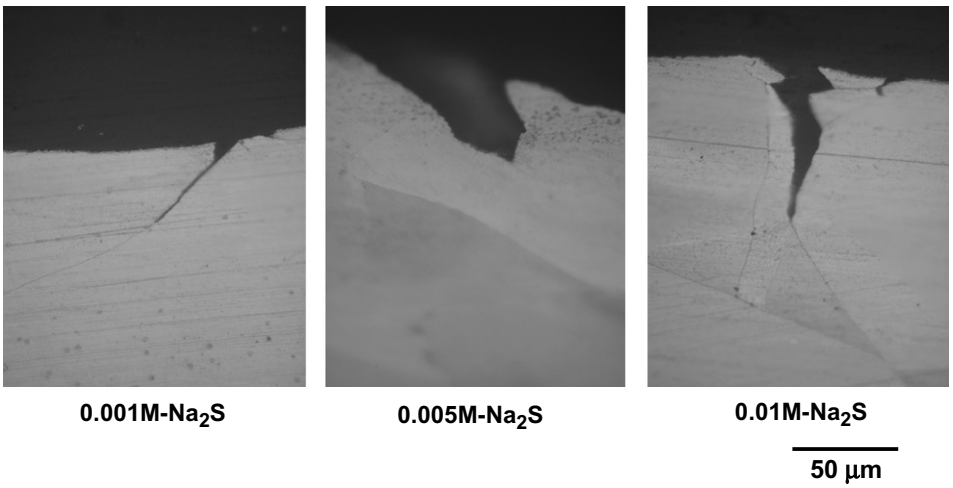

Fig. 11. Results of cross sectional observation of copper coupon after SSRT tests.

Section 3.1. The diffusion coefficient D, of 4×10^{-11} m^2/s was provisional used (see Section 3.1), and the changes in temperature with time were approximated using a step function, as 353 K for 0–1000 years; 333 K for 1000–10000 years; and 318 K for ~10000 years assuming that there is no temperature gradient in buffer material. The diffusion coefficient was corrected to the value at each temperature by an Arrhenius type equation in the same way as in Section 3.1. The D values at 353 K, 333 K and 318 K were calculated to be 1.0×10^{-10} m^2/s, 7.5×10^{-11} m^2/s and 5.9×10^{-11} m^2/s, respectively. Under fixed boundary conditions of C_1 and C_2, mass-transport approached steady state. For example, the second term of Eqs. (1) becomes nearly zero for sufficiently large t over several hundred years assuming D of 5.9×10^{-11} to 1.0×10^{-10} m^2/s and thickness, l, of 700 mm following the reference engineered barrier design [1]. Since our simulation focuses on the possibility of achieving a lifetime far exceeding 1000 years, the calculation can be simplified with a steady state equation. In this study, in order to make calculations for a more realistic geometry, the engineered barrier system was represented as a hollow cylindrical system. The total flux, Q, of sulfide for a hollow cylindrical system at steady state can be represented by following equation [14];

$$Q = 2\pi D \frac{(C_1 - C_2)t}{\ln(r_2/r_1)}, \tag{2}$$

where r_1 (=0.41 m) and r_2 (=1.11 m) are the radius of overpack and buffer material, respectively. The example of the predicted corrosion depth as a function of time is shown in Fig. 12. Provisionally, the corrosion lifetime for copper overpack was assumed to be the period for 10 mm penetration, with reference to previous assessments [1]. The predicted lifetime of copper overpack as a function of sulfide concentration is shown in Fig. 13. If the expected sulfide concentration is less than 0.001 M, copper overpack could possibly achieve a very long lifetime of ~10^4 years. The reported upper limit of sulfide concentration in typical groundwater in Japan is about 0.0003 M [8]. In this case, the expected lifetime is estimated to be

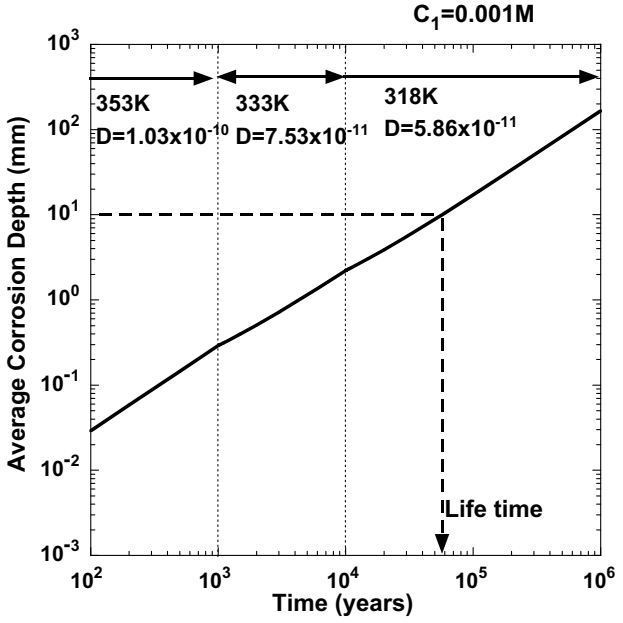

Fig. 12. An example of calculated results of average corrosion depth as a function of time.

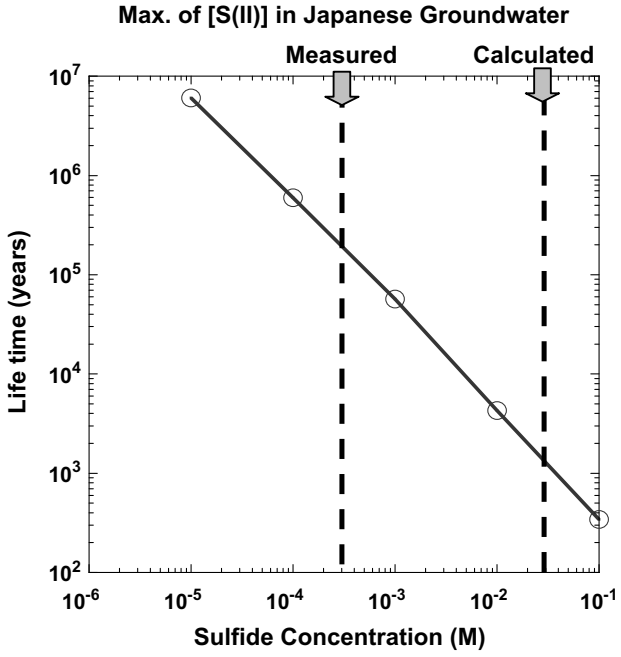

Fig. 13. Predicted corrosion lifetime of copper overpack and comparison with maximum sulfide concentration in Japanese groundwater.

over 10^5years. On the other hand, the theoretical maximum sulfide concentration has been calculated to be 100 times larger, 0.03 M from thermodynamic calculations [8]. In this case, a long lifetime cannot be expected for copper overpack. In addition, rather early penetration due to SCC could be possible under high sulfide concentrations as discussed in Section 3.2. High sulfide concentrations could be achieved by a special process such as sulfate reduction due to microbial action. Although sulfate reduction by microbial action in buffer material is not likely to occur because sulfate reducing bacteria (SRB) can hardly proliferate in compacted bentonite [17], the possibility of SRB action in groundwater outside the buffer material has not been rejected at the present time.

As discussed above, copper has the potential of achieving an extremely long lifetime depending on the environmental conditions, but it is necessary to carefully clarify those environmental conditions and their long-term evolution, in selecting copper as an overpack material.

4. Conclusions

Immersion tests and SSRT on pure copper were carried out in synthetic seawater containing Na_2S and long-term predictions of corrosion due to presence of sulfide were performed based on the model of sulfide diffusion through buffer material. The results can be summarized as follows:

Pure copper was attacked by uniform corrosion in the presence of sulfide under anaerobic conditions. The corrosion rate increased with sulfide concentration from less than 0.6 μm/y for 0.001 M-Na_2S, 2–4 μm/y for 0.005 M-Na_2S and 10–15 μm/y for 0.1 M-Na_2S.

As the results of SSRT, copper was susceptible to intergranular attack by sulfide such as selective dissolution at lower sulfide concentration and SCC at higher sulfide concentration. The threshold of sulfide concentration for the SCC initiation is likely to be in the range of 0.005–0.01 M under our experimental condition.

If the expected sulfide concentration in groundwater is less than 0.001 M, copper overpack is expected to exhibit superior corrosion resistance under anaerobic conditions since the corrosion rate will be very small and SCC will not occur. In such a low sulfide environment, copper overpack has the potential to achieve super-long lifetimes exceeding several tens of thousands years based on long-term simulations of diffusion of sulfide and corrosion of copper in buffer material.

References

[1] Japan Nuclear Cycle Development Institute, JNC TN1410 2000-003, 2000.
[2] M. Pourbaix, Atlas of Electrochemical Equilibria in Aqueous Solutions, Pergamon, 1966.
[3] D.G. Brookins, Eh–pH Diagrams for Geochemistry, Springer-Verlag, 1988.
[4] S.M. Abd El Haleem, E.E. Abd El Aal, Corrosion (NACE) 62 (2) (2006) 121.
[5] M.R. Gennero de Chialvo, A.J. Arvia, J. Appl. Electrochem. 15 (1985) 685.
[6] I.S. Escobar, E. Silva, C. Silva, A. Ubal, in: Proceedings of the Fourth International Conference Copper 99-Cobre99, vol. 1, 1999, p. 371.
[7] J. Smith, Z. Qin, F. King, L. Werme, D.W. Shoesmith, Corrosion (NACE) 63 (2) (2007) 135.
[8] M. Yui, H. Sasamoto, R.C. Arthur, JNC TN8400 99-030, 1999.
[9] N. Taniguchi, M. Kawasaki, S. Kawakami, M. Kubota, in: Proceedings of the 2nd International Workshop on Prediction of long Term Corrosion Behaviour in Nuclear Waste Systems, 2004, p. 24.
[10] N. Honma, T. Chiba, K. Tanai, JNC TN8400 99-049, 1999.
[11] H. Torii, F. Umemura, Zairyo-to Kankyo 52 (2003) 358.
[12] L.A. Benjamin, D. Hardie, R.N. Parkins, British Corros. J. 23 (2) (1988) 89.
[13] F. King, L. Ahonen, C. Taxen, U. Vuorinen, L. Werme, SKB TR-01-23, 2001.
[14] C. Crank, The Mathematics of Diffusion, Science Publications, Oxford, 1975.
[15] H. Sato, PNC TN8410 98-097, 1998.
[16] B. Case, Electrochim. Acta 18 (1973) 293.
[17] T. Nishimura, R. Wada, H. Nishimoto, K. Fujiwara, N. Taniguchi, A. Honda, JNC TN8400 99-077, 1999.